E.YA. GLUSHKO

V.E. Lashkaryov Institute of Semiconductor Physics, Nat. Acad. of Sci. of Ukraine
*(41, Prosp. Nauky, Kyiv 03680, Ukraine)*

# THE INTENSITY-DEPENDENT BAND SHIFT EFFECT IN 1D PHOTONIC CRYSTALS FOR OPTICAL SIGNAL PROCESSING

UDC 539

*The electromagnetic spectrum of an optically linear 1D glass-air comb photonic crystal is considered both in the cases of total internal reflection and open incidence. The bandgap-reflection/angular-frequency diagram is calculated for a glass/air comb in the infrared and visible regions. The effect of intensity-dependent reflection arising when a light beam passes through a nonlinear film covering the linear photonic crystal is investigated. The shift of photonic bands is analyzed for silica glass structures containing nonlinear inclusions, and two possible schemes of optical signal processing in a comb-like resonator are discussed.*

*K e y w o r d s:* all-optical signal processing, all-optical logic gates, optically nonlinear materials, photonic bandgap materials.

## 1. Introduction

The present-day informational and communication networks demand the growing multimedia online services, multiflow real time data transport, and faster access to resources. These trends cause a demand to develop extremely high-speed telecommunication systems with a processing capacity, which should be increased from the today's several tens of gigabytes per second to several Tb/s. One more challenge to be answered in the future is the creating of power computers called to solve global problems of climate change, planetary ecology, Earth's safety, industry, economics, science, and technique. Therefore, the all-optical principle in logical devices for the optical computing, optical associative memories, and optical interconnections will allow higher working frequencies in the signal processing, small energy losses, and practically unlimited possibilities to organize the parallel operating of signals [1–8]. The all-optical concept implies that the most responsible stages of signal processing operations are performed without usage of electronic or others nonoptical mechanisms. The reason for a higher efficiency of the all-optical signal processing in comparison with mixed ways is in the obvious axiom that each signal transformation from one physical form into another one decreases the common speed of a signal passing through the device. Thus, the implementation of the all-optical approach in computing devices may have a great importance for the development of the next generation of computers. The all-optical devices implemented into the modern communicational world should solve various tasks of giant dataflow processing and computing.

Silicon glass is one of the perspective materials for the fabrication of complex integrated structures for the optical signal processing in the visible region [6–8]. A class of 1D ordered structures is presented by material/air comb-shaped photonic crystals [9]. The comb-like silica glass photonic crystals may serve as optical resonators with well-expressed bands and gaps in the region of total internal reflection (TIR) and with reflection/transmission windows in the outer region of angles both for infrared and visible spectral ranges. Here, we consider a way of the all-optical signal processing based on a photonic bandgap structure

built on the base of a silica glass comb matrix with optically nonlinear layers on both sides. Due to the nonlinearity, the band position undertakes shift – the quasiband shift effect – which leads to a strong deviation in the transmission and the reflection of a light signal in dependence on its intensity. This allows one to perform the main function of an all-optical adder to transform the sequence of physically added optical signals into a sequence of binary signals with a corresponding shift of digital units. Meanwhile, in the physical literature, the waveguide way to control optical signals is widely spread. As usual, a photonic crystal plays both the role of a perfectly reflecting surrounding and a technological medium to produce waveguide channels.

In this paper, we concentrate on the physical grounds and the general principles of all-optical signal processing with the use of a one-dimensional photonic crystal covered with a nonlinear film. The choice is conditioned by the advantages of layered ordered structures such as technological simplicity, well-expressed bandgap structure, good integrative perspectives, and high prognostic and analytical properties peculiar to 1D systems.

## 2. Photonic Crystal Resonators and Standing Wave States

The typical 1D photonic resonator shown in Fig. 1 includes a photonic crystal supplied with special input-output prism 3 to excite standing waves inside the structure. The resonator consists of alternating layers of materials 1 and 2 composing the structure period and of the covering layer **a** made of an optically nonlinear material. The input-output prisms of the same nonlinear material serve to control the band edge position in dependence on the beam intensity. The system geometry presented in Fig. 1 gives an opportunity to excite the electromagnetic modes inside the area of total internal reflection of a 1D photonic crystal resonator.

We now consider the electromagnetic field in a photonic crystal. If a $p$-polarized wave propagates in a binary 1D layered structure consisting of $N$ periods of two contacting materials (plus one end layer of material 1), then the solution for the field $\mathbf{E}$ can be sought in the general view as

$$\mathbf{E}_j = (\sin\theta_j, \cos\theta_j)\mathbf{A}_j e^{i\mathbf{k}_j\mathbf{x}} + \\ +(\sin\theta_j, -\cos\theta_j)\mathbf{B}_j e^{-i\mathbf{k}_j\mathbf{x}}, \qquad (1)$$

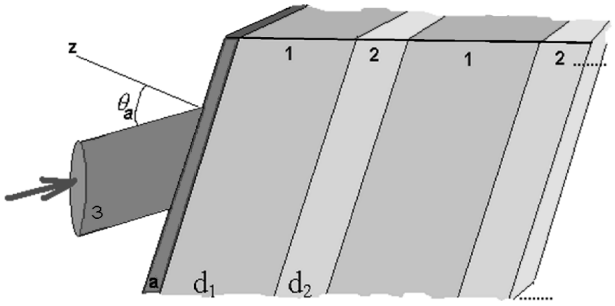


***Fig. 1.*** Excitation of intrinsic modes in a 1D photonic crystal resonator. *1* and *2* – optically transparent materials of the periodic structure; **a** – covering nonlinear layer (doped glass); *3* – input prism; $\theta_a$ – incident angle through the input; $d_1$ and $d_1$ – layer thicknesses; z-direction is perpendicular to layers

where the wave vector $\mathbf{k}_j = k_j(\cos\theta_j, -\sin\theta_j)$, $k_j = 2\pi/\lambda_j$, and $\lambda_j$ is the wavelength in the $j$-th layer. Following the transfer matrix approach developed in [10] for the field amplitudes $\mathbf{A}_j$ and $\mathbf{B}_j$ with regard for the continuity of the tangential component of the electrical field and the normal component of the induction, we obtain the chain of $2N+1$ matrix equations

$$\begin{cases} \widehat{M}_l \begin{pmatrix} A_l \\ B_l \end{pmatrix} = \widehat{L}_1 \begin{pmatrix} A_1 \\ B_1 \end{pmatrix} = \widehat{M}_1^{-1} \cdot \widehat{L}_2 \begin{pmatrix} A_2 \\ B_2 \end{pmatrix} = \\ = \widehat{M}_2^{-1} \cdot \widehat{L}_3 \begin{pmatrix} A_3 \\ B_3 \end{pmatrix} = ... = \widehat{M}_{2N}^{-1} \cdot \widehat{L}_{2N+1} \begin{pmatrix} A_{2N+1} \\ B_{2N+1} \end{pmatrix} = \\ = A_r \widehat{M}_{2N+1}^{-1} \cdot \widehat{L}_r \begin{pmatrix} \cos\theta_r \\ \varepsilon_r \sin\theta_r \end{pmatrix}. \end{cases} \qquad (2)$$

In the case of beam external incidence, the amplitude of the incident wave $A_l$ should be taken equal to 1, whereas $A_l = 0$ in the total internal reflection case. Due to the unboundedness of the right medium, $B_r = 0$. To solve the chain of equations (2), we introduce the transfer matrix $\widehat{\Lambda}$, which arises during the reduction procedure: $\widehat{\Lambda} = \widehat{L}_1 \widehat{M}_1^{-1} \widehat{L}_2 \widehat{M}_2^{-1} = \widehat{\Lambda}_1 \widehat{\Lambda}_2$, where

$$\widehat{M}_l = \begin{pmatrix} \cos\theta_l & -\cos\theta_l \\ \varepsilon_l \sin\theta_l & \varepsilon_l \sin\theta_l \end{pmatrix}, \quad \widehat{\Lambda}_s = \begin{pmatrix} \mu_s, \nu_s \\ \lambda_s, \mu_s \end{pmatrix}, \qquad (3)$$

and $\theta_l$, $\theta_r$ are incident angles in media surrounded the structure. The transfer matrix elements for the $s$-th layer are as follows:

$$\mu_s = \sin 2\theta_s \, \cos k_{sz} d_s/\Lambda, \\ \lambda_s = -2i \sin^2\theta_s \, \sin k_{sz} d_s/\Lambda, \qquad (4) \\ \nu_s = -2i \cos^2\theta_s \, \sin k_{sz} d_s/\Lambda.$$

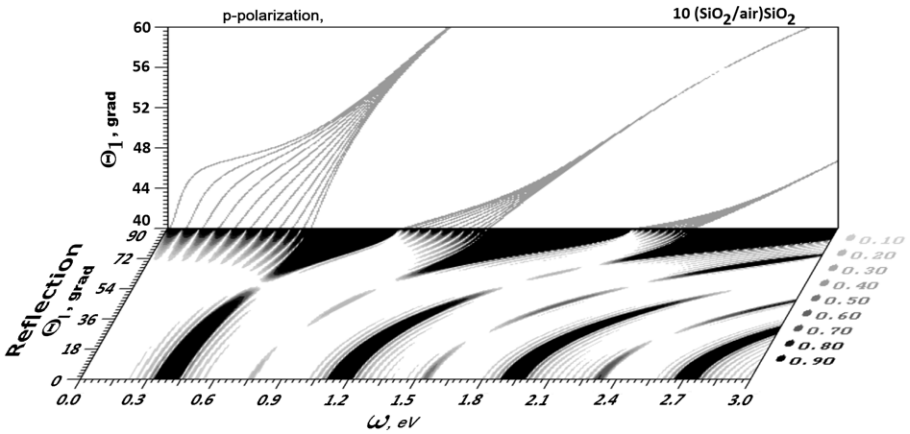


***Fig. 2.*** Bandgap-reflection angular-wavelength diagram for a glass/air comb. 10-period 1D $(SiO_2/air)_{12}$ $SiO_2$ structure. Vertical panel: inside the total internal reflection area; $40^\circ < \theta_1 < 60^\circ$, $d_1 = 0.5$ $\mu$m, $\varepsilon_1 = 2.4$, $SiO_2$ layer thickness, $d_2 = 0.825$ $\mu$m, air voids thickness, $\varepsilon_2 = 1.0$. Horizontal panel: The angle-frequency reflection diagram. The grey color gradation is given by the right column on the horizontal panel: saturated grey, $0.9 < R < 1$, white, $0 < R < 0.1$

Here, the index $s = 1, 2$ numbers the layers inside the period, $k_1$, $k_2$ are amplitude-independent field wave vectors inside the layers. The constant $\Lambda$ in (4) is the transfer matrix $\widehat{\Lambda}$ determinant. For standing waves in the TIR area, $\theta_r = \theta_l$, $\cos\theta_l = i\overline{\cos\theta_l}$. Relations (2) yield immediately the dispersion equation

$$\overline{\cos\theta_l}\left[(\widehat{\Theta}^N)_{21}\cos\theta_r + (\widehat{\Theta}^N)_{22}\sin\theta_r\right] + \\ +\varepsilon_l\,\overline{\sin\theta_l}\left[(\widehat{\Theta}^N)_{11}\cos\theta_r + (\widehat{\Theta}^N)_{12}\sin\theta_r\right] = 0, \qquad (5)$$

where matrix elements $()_{\rm st}$ are taken from the matrix $\widehat{\Theta}^N$

$$\widehat{\Theta}^N = \widehat{\Lambda}^N\widehat{L}_1\widehat{M}_1^{-1}, \qquad (6)$$

which includes the $N$-th power of the transfer matrix $\widehat{\Lambda}$ and takes the right and additional layers of material 1 into account.

We have calculated the eigenmode structure ($A_l = 0$ in (2)) of TH-polarized plane waves trapped inside the photonic crystal by TIR in dependence on the incident angle, number of periods, and layer widths for various frequency intervals. It is worth to note that these standing modes are unattainable for external light sources, but may be activated with the use of special prism inputs contacting with nonlinear layers covering the resonator (Fig. 1).The external incidence of a light beam in the case where the input prism is absent was also analyzed. In Fig. 2, a united bandgap-reflection angle vs the photon energy for a 10-period glass/air comb resonator is shown. The structure of band eigenmodes of the photonic crystal for the parameters $d_1 = 0.5$ $\mu$m, $d_2 = 0.825$ $\mu$m for the angular interval of total internal reflection $40^\circ < \theta_1 < 60^\circ$ is shown in the upper part of the graph for the photon energy interval ranging from 0 to 3.0 eV. Three bands each containing 11 modes are present in the shown interval of frequencies. The local/surface modes are absent in aired comb-like photonic crystals.

The 2D gray color gradation diagram for the reflection of a TH-polarized plane wave from the photonic resonator at arbitrary incident angles $\theta_l$ was calculated in the framework of the external problem. The result is shown on the horizontal panel of Fig. 2 for angles $\theta_l$ ranging from $0^\circ$ to $90^\circ$. The interval (0.9, 1) of the most intense reflection is shown there by saturated grey color. The white colored regions of the horizontal panel correspond to a weak reflection in the interval from 0 to 0.1. The boundary between the TIR angular area ($\approx 40.18^\circ$) and the area of external incidence ($90^\circ$) shows the transfer from a comb of peaks of transmission at $\theta_l \approx 90^\circ$ lying on the horizontal panel to the beginning of internal modes shown at the vertical panel.

The generalized dispersion equation (5) is most convenient to analyze the standing modes in a 1D photonic crystal. In the general case, four types of modes exist in 1D photonic crystal resonators: trans-

mitted modes; waveguide-transmitted modes ($\varepsilon_2 < \varepsilon_1$); pure waveguide modes ($\varepsilon_1 < \varepsilon_2$); and local (surface) modes inside the gaps.

The analysis of the dispersion equation (5) shows that if the resonator is placed into a medium coinciding with one of the materials which form the structure period, the local surface modes (if exist) vanish. One more case: if the intrinsic optical contrast of the resonator is not too high, like that for glass/glass layered structures, then waveguide modes are also absent. It is worth to note that the full solution of the problem for a field including the field distribution inside the resonator can be obtained after substituting the amplitudes found from (2) in (1) for a given eigenvalue $\omega_j$.

Combining the parameters $d_1$, $d_2$ for the taken material (silica glass), one can obtain a lot of possibilities to choose working points. Due to the existing scaling symmetry of equations (2) and (5), the band structure does not change when the transformations $\omega \to t\omega$ and $d_s \to d_s/t$ are performed, where $t$ is a constant, and $s$ indicates the material of the $s$-th layer. The reason is that the arguments of sine and cosine in transfer matrix elements (4) are $k_s d_s$, where $k_s$ is proportional to the frequency $\omega$. This means that, for the band structure shown in Fig. 2 (upper part), the absolutely same one may be observed for $d_1 = 5$ $\mu$m, $d_2 = 8.25$ $\mu$m but in the wavelength interval ranging from 0 to 0.3 eV. The existing scaling property allows one to easily recalculate the photonic crystal parameters needed for the given laser frequency of a signal.

## 3. Shift Band Effect in Finite Photonic Crystals for Signal Processing

The most attractive for the signal control purpose are nonlinear materials uniting a strong nonlinearity with small relaxation times. The nonlinear properties of CuCl films and Cu&Ag nanoparticle doped glasses were considered in [11, 12]. We suppose that the deviation of the refraction index dependence for an isotropic medium is proportional to the light intensity $\Delta n_l \sim I(\omega)$, where $\omega$ is the frequency, and the nonlinear coefficient of proportionality $q_2$ is measured in cm$^2$/kW. It is worth to note that the discussed phenomenon of a shift of bands is caused by the Kerr effect. When a beam passes through the nonlinear $a$-layer (Fig. 1) into the bulk of the optically linear photonic crystal, its incident angle at the $a$-layer/resonator boundary changes, by depending on the beam intensity (band quasishift effect). Though the angle position of the band edge in a linear photonic crystal at a given frequency is fixed, a dependence arises between the beam intensity and the angle of entrance into the bulk. Therefore, the reflectance in a vicinity of the band edge can be significantly changed depending on the light intensity or, what is the same, on the incident angle at the $a$-layer/resonator boundary. Two possible variants exist in the considered geometry with a nonlinear coating layer and the positive nonlinear coefficient $q_2$: signal processing in a vicinity of the short-wavelength edge of a reflection window (T-scheme) or near the long-wavelength edge of a reflection window (R-scheme). The quasishift effect takes place in a linear photonic crystal covered with an optically nonlinear layer. As to the truly band shift effect, it arises if a beam passes through the optically nonlinear photonic crystal. It is easy to understand that the band shift effect and the band quasishift effect have opposite signs. In the second case, the reflection windows shift to right on the frequency scale, as it may be concluded from Fig. 3.

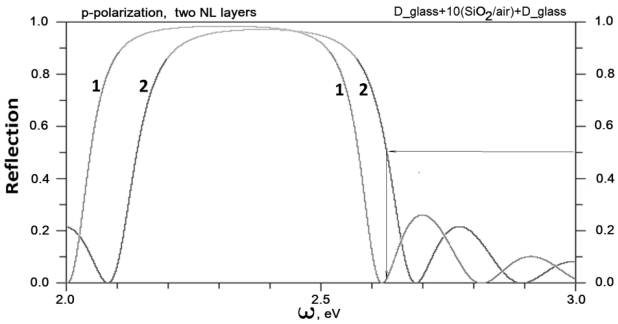


***Fig. 3.*** Intensity-dependent shift of the reflection window. Nonlinear doped glass [11, 12] covered the $SiO_2$/air 10-period comb photonic crystal. R-scheme of signal processing. $\theta_a = 30°$, angle of incidence inside the $a$-layer, $\varepsilon_1 = 1.924$, $\theta_1 = 30°$, *1*, reflection frequency dependence at the beam intensity "one" $I_0 = 6.0 \times 10^4$ kW/cm$^2$, *2*, the same for beam intensity "two" $2I_0$, $q_2 = 3.0 \times 10^{-7}$ cm$^2$/kW, arrows show the half-reflection at the working blue photon energy $\omega_0 = 2.628$ eV ($\lambda_0 = 0.472$ $\mu$m)

The intensity dependence of a selected reflection spectrum fragment calculated by relations (2) for the energy interval (2.0–3.0) eV is shown in Fig. 3. We assign here the light beam angle inside the doped glass

$a$-layer $\theta_a = 30°$, $\varepsilon_a = 1.924$ [11, 12], beam intensity "one" equals to $I_0 = 5.0 \times 10^4$ kW/cm$^2$, and nonlinearity coefficient $q_2 = 3.0 \times 10^{-7}$ cm$^2$/kW. Choosing the number of layers, thicknesses, and angle of incidence onto the logic cell (see Fig. 1), one can find the suitable magnitude of reflection at a given working frequency $\omega_0$. In the so-called R-scheme of all-optical signal processing, the beam "one" has a perfect transmission through the resonator, whereas signal "two" is fully reflected by the system. Here, we investigate the system satisfying the condition of half-reflected signal "two". At the chosen working wavelength $\lambda_0 = 0.472$ $\mu$m (blue light), the comb system ($d_1 = 0.5$ $\mu$m, $d_2 = 0.825$ $\mu$m) consisting of 10 glass/air periods and covered on both sides with nonlinear layers $d_a = 1.0$ $\mu$m gives the perfect transmission of signal "one" (Fig. 3, curve *1*, vertical arrow), whereas the reflection coefficient $R = 1/2$ for signal "two". Such a kind of half-R scheme of processing successfully resolves the problem of output extra energy rejection, when a physically added signal "two" passes a logic gate: output gives the demanded signal "one" (Fig. 3, curve *2*, horizontal arrow), which should be redirected as a "shifted bit" to the more significant bit position. This subject will be discussed below. It is worth to note that the so-called T-scheme of processing, when signal "one" should be absolutely reflected by the logic cell, has some difficulties for the system under consideration due to the weak intensity dependence of the band bottom. As to the proposed half-R scheme, it is extremely sensitive to the number of layers in the photonic crystal resonator: for $N = 11$ (or 12), the semireflection in a vicinity of reflection window's edge is destroyed at any working frequencies. If the TIR regime is chosen for the signal processing, a more rigid demand for the number of periods $N > 12$ should be realized to supply the absolute reflection and transmission for chosen working frequencies in vicinities of the band edge. The angular properties of the signal processing area is of importance as well. In view of the finite number of modes inside the band, the angle of processing $\theta_a$ must satisfy the condition of possible maximal density of states.

In fact, the nonlinear influence of the active $a$-layer on the resonator band gap structure should not be understood in a direct sense. Though the covered active layer is thin comparatively with the volume of PhCr, the change of the signal intensity leads to a sufficient change in the incidence angle of the wave coming from the nonlinear layer into the linear photonic crystal. The evaluation of the nonlinear solution for electromagnetic waves in the $a$-layer made in [10] has shown that a deviation of the wave profile from the harmonic shape may be neglected if $\Delta n_l \leq 0.01$. Then, in order to avoid the unwanted instability or wave shape nonharmonicity, it is enough to take light intensities not exceeding essentially $10^7$ kW/cm$^2$. Therefore, one can suppose that the chosen light intensity $10^4$–$10^5$ kW/cm$^2$ does not lead to the bistability effects and does not influences substantially the harmonic character of the wave. In our case, the only manifestation of a nonlinearity is a weak modulation of the refractive index.

## 4. Summary

In conclusion, the concept of all-optical signal processing based on a linear 1D photonic crystal with nonlinear cladding layers is presented. Due to the better resonator properties of layered photonic structures in comparison with the waveguides, the approach under consideration gives the significant decrease in working intensities from the conventional $10^6$ kW/cm$^2$ to $10^4$ kW/cm$^2$. The conclusion can be also made that 1D photonic crystals, being more optically contrast systems [13], are more suitable in all-optical signal transformation devices, whereas the two-dimensional structures may be used there as the integrating medium with communicating waveguides and ray-guides, which allows one to miniaturize the signal transformation in logical gates and adders. However, several physical and technical circumstances should be cleared to realize experimentally the proposed concept:

– Band shift effect measuring technique;

– A technique of excitation of band states under total internal reflection;

– A technology of the integrated logic cells based on photonic crystal resonators;

– High optical strength lossless materials for the linear part of logic cells;

– Fast nonlinear materials for the covering of a photonic crystal resonator;

– Integrated waveguide technology to create the body of a logic cell.

1. J.-M. Brosi, *Slow-Light Photonic Crystal Devices for High-Speed Optical Signal Processing* (Univ. Karlsruhe, Karlsruhe, 2010).

2. F. Yanik, S. Fan, M. Sojiacic, and J.D. Jannopoulos, Opt. Lett. **28**, 2506 (2003).
3. K.A. Rutkowska, D. Duchesne, M.J. Strain, R. Morandotti, M. Sorel, and J. Azaña, Optics Express **19**, 514 (2011).
4. H. Inoue, K. Tanaka, I. Tanahashi, T. Hattori, and H. Nakatsuka, Jpn. J. Appl. Phys. **39**, 5132 (2000).
5. B.C. Jacobs, C.N. Weiler, J.P. Maranchi, C.R. Sprouse, D.G. Lucarelli, and B.G. Rayburn, John Hopkins APL Technical Digest **30**, 346 (2012).
6. J. van Howe and Ch. Xu, J. Lightwave Technology **24**, 2649 (2006).
7. P. Russell, IEEE LEOS Newsletter **10**, 11 (2007).
8. G. Brambilla, J. Opt. **12**, 043001 (2010).
9. E.Ya. Glushko, Proc. SPIE **6903**, 69030G (2008).
10. T. Hattori, Jpn. J. Appl. Phys. **41**, 1349 (2002).
11. A.L. Stepanov, Rev. Adv. Mat. Sci. **27**, 115 (2011).
12. E.Ya. Glushko, Eur. Phys. J. D **66**, 36 (2012).

Received 23.05.12

*Є.Я. Глушко*

ЗАЛЕЖНИЙ ВІД ІНТЕНСИВНОСТІ ЕФЕКТ ЗСУВУ ЗОН В 1D ФОТОННИХ КРИСТАЛАХ ДЛЯ УПРАВЛІННЯ ОПТИЧНИМИ СИГНАЛАМИ

Р е з ю м е

Розглянуто електромагнітний спектр оптично лінійного 1D фотонного кристала як в області повного внутрішнього відбивання, так і у випадку входу світла в фотонний кристал без заломлюючих призм. Для гребінки скло–повітря проведено розрахунок зонної структури та коефіцієнта відбиття в залежності від кута падіння та частоти в інфрачервоному та видимому діапазонах. Також досліджено ефект залежності відбивання пучка світла, що проходить послідовно крізь нелінійну плівку та фотонний кристал, від інтенсивності світла. Проведено аналіз зсуву фотонних зон у скляних структурах, які містять нелінійні включення та обговорено дві схеми управління оптичними сигналами в гребінчастому резонаторі, покритому оптично нелінійною плівкою.

*Е.Я. Глушко*

ЗАВИСИМЫЙ ОТ ИНТЕНСИВНОСТИ ЭФФЕКТ СДВИГА ЗОН В 1D ФОТОННЫХ КРИСТАЛЛАХ ДЛЯ УПРАВЛЕНИЯ ОПТИЧЕСКИМИ СИГНАЛАМИ

Р е з ю м е

Рассмотрен электромагнитный спектр оптически линейного 1D фотонного кристалла как в области полного внутреннего отражения, так и для случая входа света в фотонный кристалл без преломляющих призм. Для гребенки стекло–воздух проведен расчет зонной структуры и коэффициента отражения в зависимости от угла падения и частоты в инфракрасном и видимом диапазонах. Исследован эффект зависимости отражения пучка света, который проходит последовательно через нелинейную пленку и фотонный кристалл, от интенсивности света. Проведен анализ сдвига фотонных зон в стеклянных структурах, которые содержат нелинейные включения и обсуждаются две схемы управления оптическими сигналами в гребенчатом резонаторе, покрытом оптически нелинейной пленкой.